Determining the domain of stable human sit-to-stand motions via controlled invariant sets and backward reachability

Daphna Raz[1], Liren Yang[2], Brian R. Umberger[3], and Necmiye Ozay[1]

***Abstract*— Falls during sit-to-stand are a common cause of injury. The ability to perform this movement with ease is itself correlated with a lower likelihood of falling. However, a rigorous mathematical understanding of stability during sit-to-stand does not currently exist, particularly in different environments and under different movement control strategies. Having the means to isolate the different factors contributing to instability during sit-to-stand could have great clinical utility, guiding the treatment of fall-prone individuals. In this work, we show that the region of stable human movement during sit-to-stand can be formulated as the backward reachable set of a controlled invariant target, even under state-dependent input constraints representing variability in the environment. This region represents the 'best-case' boundaries of stable sit-to-stand motion. We call this the *stabilizable region* and show that it can be easily computed using existing backward reachability tools. Using a dataset of humans performing sit-to-stand under perturbations, we also demonstrate that the controlled invariance and backward reachability approach is better able to differentiate between a true loss of stability versus a change in control strategy, as compared with other methods.**

I. INTRODUCTION

Falls that occur during daily activities are a leading cause of injury and death in the geriatric population [1], and can cause harm across the lifespan [2], [3]. Within hospital settings, up to one million patient falls occur annually [4]. Mitigating or preventing falls would therefore have a measurable benefit to public health, including the reduction of healthcare costs [5]. However, the underlying mechanisms of falling are not well-understood. They are particularly understudied in the case of non-ambulatory activities such as sit-stand transitions, which include sit-to-stand and stand-to-sit movements. Sit-to-stand is performed as frequently as 60 times per day [6], and requires a larger range of motion than walking, coupled with sufficient muscle power and appropriate limb coordination [7]. Falls occur frequently during sit-stand transitions, particularly in the elderly population and those who have experienced strokes [8]. A number of reasons can be ascribed to these falls, such as limb collapse, weakness, a failed control strategy, or environmental factors such as a slippery floor [9], [10]. However, it is difficult to isolate each of these factors experimentally. Understanding how each factor contributes to instability could guide treatment; for some patients, a focus on strength training may be necessary, while others may require coaching in new control strategies.

Not only do falls occur frequently during sit-to-stand, but sit-to-stand performance is itself correlated with the likelihood of falling during other activities [11]. A mathematically rigorous understanding of the factors contributing to stability during sit-stand motions would therefore be of value and could have great clinical utility. Progress could be made in areas such as fall prediction and prevention [12], design of rehabilitation protocols [13], tracking progression of degenerative movement disorders [14], and improving the safety of assistive devices such as prostheses [15], [16]. In this human context, we consider stable movements to be those that are not prone to falling. It is unclear whether classical, Lyapunov-like notions of stability about an equilibrium or nominal trajectory are able to fully encompass such movements.

Several methods have been proposed to assess the stability of human movements. Early work considered the projection of the body center of mass (CoM) position onto the plane parallel to the base of support (BoS), defined by the location of the feet on the ground [17]. However researchers observed that this definition is too restrictive, as it is possible for humans to stablize when the CoM position is outside of the BoS, for example when walking. To detect stable configurations outside of the BoS, researchers proposed considering CoM velocity [18]. Using an actuated nonlinear inverted pendulum model and state-dependent input constraints on the torque at the ankle, they computed a stable region of the CoM position-velocity phase plane. Maximum and minimum velocities were computed for each CoM position such that the pendulum could still be restored to upright standing. Bounds were obtained by simulation, with initial conditions selected via a computationally expensive iteration over the entire state space [18]. Constraints were enforced by assuming a supervisory controller, and only the portion of the phase plane corresponding to forward moving/anterior velocity was computed.

Building on this work, Hof et al. derived bounds on the stable region using a linearized model [19]. This method, the extrapolated center of mass, or XCoM, has become one of the most popular approaches in the biomechanics literature. However, XCoM can only be used with a linearized inverted pendulum model, and does not incorporate general state-dependent torque constraints. More recent similar work has

[1]Robotics Institute, University of Michigan, Ann Arbor, MI 48109, USA. {daphraz,necmiye}@umich.edu

[2]School of Artificial Intelligence and Automation, Huazhong University of Science and Technology, Wuhan 430074, China lirenyang@hust.edu.cn.

[3]School of Kinesiology, University of Michigan, Ann Arbor, MI 48109, USA. umberger@umich.edu

This work was supported by the National Institute of Biomedical Imaging and Bioengineering of the NIH under Fellowship Number F31-EB032745. This work was also supported by NSF Award CPS-1931982.

generalized the framing of this problem to multilink models [20]. The upper and lower boundaries of the stable regions are estimated by solving two highly constrained nonlinear optimization problems for every point in a gridded statespace via sequential quadratic programming. This approach is more general, but it provides only locally optimal solutions.

Much research in controls focuses on stability during walking, using constructs that depend on periodicity, foot placement, or require large amounts of data [21]. Recently, researchers have characterized the boundaries of stable walking by finding the set of initial conditions from which falls can be avoided while specified goals can be reached [22], [23]. To compute similar regions in continuous time for nonperiodic behaviors, it is possible to use tools for computing the backward reachable set, a concept which we treat more thoroughly later in the text. In brief, given a continuous time dynamical system and a goal region in the state space, the backward reachable set is the set of all states from which it is possible to reach the goal region, within a certain time horizon.

The approach in [24] uses experimental data to construct an individualized 'stability basin', or backward reachable set when a parametrized control strategy is fixed and learned from experimental sit-to-stand data. The stability basins can be used to classify sit-to-stand performance such that sit-to-stand trajectories resulting in a step or fall backward tend to exit the basins while successful trials do not. This method provides proof of concept for using backward reachability tools. It is a novel approach for studying the effect control strategies may have on stability during a specific movement. However the basins exclude some biomechanically stable configurations. Furthermore, state-dependent constraints on the input are not considered in this application, and large amounts of experimental data are required.

Notably, none of the aforementioned methods offer a guarantee that the computation converges to the region consisting of *all* states from which it is possible to reach a properly defined target set. Such guarantees are powerful, because they provide a rigorous way to differentiate between a situation where a fall is inevitable, and a situation where a movement strategy exists that maintains some form of stability. Currently, no method exists that can compute such regions for sit-stand transitions over a range of constraints, environmental factors, physiological factors, and control strategies. There is thus a need for a method that would allow us to study how each of these factors affect human stability in a systematic manner, something that is currently not possible.

In this paper, we propose such a method, by formally characterizing the *stabilizable region* of human movement to be the backward reachable set of a controlled invariant target set. We consider a target set that is typically used in biomechanics literature and show that this set is controlled invariant. Controlled invariance is a nice property for a target set to have since it means there exists a control strategy that ensures every trajectory starting from the set will stay in it indefinitely. It captures the desired static behavior under proper balancing after the sit-stand motion is finished. The backward reachable set, on the other hand, consists of all the states that can be driven into the controlled invariant goal set in finite time with some controlled strategy. Therefore, it captures the sit-stand phase. Notably, in this specific setting, the backward reachable set itself can be shown to be controlled invariant. This hence provides a similar safety guarantee as the viability kernel does in [22].

Controlled invariance and backward reachability allow us to develop a general formulation that is not model- or task- dependent, and can be used for nonlinear, hybrid, multidimensional, and aperiodic systems. It also provides a way to clearly assert whether a failure is due to a specific bad control strategy or just fundamentally inevitable. Under this framework, we further include parametrized state-dependent input constraints. This enables exploration of how changes in the environment, such as a slippery floor, may affect stability. For the case of a sit-stand model, we show that we are able to easily compute stabilizable regions over a range of environment and model parameters. Under nominal non-slippery conditions, our stabilizable region corresponds to the same regions of the state space as [18] and [20], as desired. Lastly, we perform a preliminary validation with a dataset of able-bodied adults performing sit-to-stand using their natural control strategy [24].

II. PRELIMINARIES

Consider the continuous time, possibly nonlinear system

$$\dot{x} = f(x, u) \tag{1}$$

where the system state is $x \in X$, and $u \in U \subset \mathbb{R}^m$ is the input. With a slight abuse of notation, we will also use $u : [0, \infty) \to U$ or simply $u(\cdot)$ to represent an input signal. We will assume f and $u(\cdot)$ are sufficiently regular to guarantee the existence and uniqueness of solutions within X (which is typically taken as a subset of $\mathbb{R}^n$). Let $\mathcal{U}$ be the set of all input signals, we use $\varphi(t; x_0, u)$ to denote the system's solution at time t from initial condition x_0 under input signal $u(\cdot) \in \mathcal{U}$.

A *controlled invariant set* for system (1) is a subset of the state space where there exists an appropriate control input $u(\cdot) \in \mathcal{U}$, such that the system state can remain within that set for all time. We use the following formal definition.

Definition 1. $\Omega \subset X$ is a *controlled invariant set* if for every initial state $x_0 \in \Omega$, there exists an input signal $u(\cdot) \in \mathcal{U}$ such that $\varphi(t; x_0, u) \in \Omega$ for all $t \in [0, \infty)$.

Now suppose we have a target set $S \subset X$. The set of all $x \in X$ for which there exists a control input such that S can be reached within some finite time horizon is the backward reachable set of S.

Definition 2. Let $S \subset X$ and $T \in \mathbb{R}^+$. Then $\mathcal{G}_T(S)$, the *maximal backward reachable set* of S at time T, is

$$\mathcal{G}_T(S) := \{x \in X \mid \exists u(\cdot) \in \mathcal{U} \, s.t. \, \varphi(T; x, u) \in S\}. \tag{2}$$

The backward reachable set $\mathcal{G}_T(S)$ defined in equation (2) is *maximal* in the sense we allow the full freedom to choose

the control input $u(\cdot)$. In many applications, a control law is fixed, e.g., $u(t) = Kx(t)$, and one can define a set $\underline{\mathcal{G}}_T(S)$ that consists of all the backward reachable states of S under this specific control law. In that case, we have $\underline{\mathcal{G}}_T(S) \subseteq \mathcal{G}_T(S)$ but $\underline{\mathcal{G}}_T(S)$ is not necessarily maximal due to the restriction on $u(\cdot)$.

Definition 2 does not require that target S be controlled invariant. However, notice that if it is, then the maximal backward reachable is controlled invariant by construction.

Fact 1. *The maximal backward reachable set of a controlled invariant set is itself controlled invariant (see, e.g., [25]).*

Proposition 1. *Assume a system as defined in* (1). *Let $S \subset X$ be controlled invariant. Then $\mathcal{G}_{t_1}(S) \subset \mathcal{G}_{t_2}(S)$ for all t_1, $t_2 \in \mathbb{R}^+$ with $t_1 < t_2$.*

Proof: Let $x \in \mathcal{G}_{t_1}(S)$. Then there exists a controller $u_1(\cdot)$, s.t. $\hat{x} = \varphi(t_1; x, u_1) \in S$. Because S is invariant, there must also exist a controller $u_0(\cdot)$ that forces the system to remain in S for all time, when starting from initial condition $\hat{x}$. Define a controller $u_2(\cdot)$, such that $u_2(t) = u_1(t)$ when $t \in [0, t_1]$ and $u_2(t) = u_0(t - t_1)$ when $t \in (t_1, t_2]$. Then $\varphi(t_2; x, u_2) \in S$, therefore $x \in \mathcal{G}_{t_2}(S)$. □

We can also define the *maximal backward reachable tube* of a set $S \subset X$ over a time horizon $[0, T]$ as $\mathcal{G}_{[0,T]}(S) = \cup_{t\in[0,T]}\mathcal{G}_t(S)$.

Corollary 1. *If the target set S is invariant, then $\mathcal{G}_{[0,T]}(S) = \mathcal{G}_T(S)$.*

A nice consequence of this corollary is that to compute $\mathcal{G}_{[0,T]}(S)$, it is not necessary to compute the entire backward reachable tube, but rather only the backward reachable set at time T. There exist several tools that can compute controlled invariant sets or backward reachable sets. In particular, a few methods [26], [27] can asymptotically achieve maximality for generic nonlinear systems, at the cost of scalability; whereas other methods are more efficient but either rely on extra assumptions on the dynamics [28], [29], [30], or only give conservative under-approximations that are not necessarily maximal [31], [32], [33]. In our application we use Hamilton Jacobi reachability [27], which is well suited for low dimensional, nonlinear systems. We describe how we apply this method to our system in section IV-C.

III. PROBLEM STATEMENT

In [18], [19] the stable region of human movement is defined with respect to the body center of mass (CoM) position and velocity projected onto the $x-$axis (fore-aft direction in the sagittal plane, as shown in Figure 1). Given an initial CoM velocity, a CoM position is considered stable if it is still possible for the CoM to come to a full stop, with the x-coordinate of the CoM (CoM_x) inside the base of support (BoS). Recall that the BoS is the location of foot contact with the ground.

Let us call the set of configurations such that CoM_x is in the BoS at zero velocity the *target set*. We wish to:

1) Show that this target set is controlled invariant under the appropriate constraints on the dynamics.

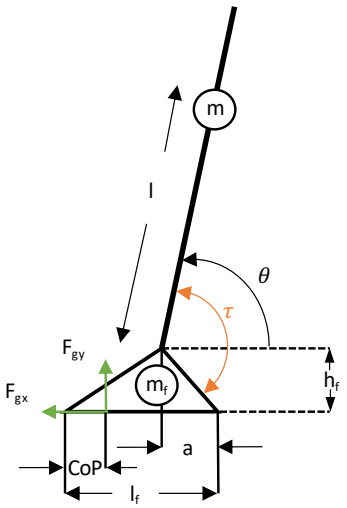

Fig. 1: Two-link model. F_{gx} and F_{gy} are the ground reaction forces, m and m_f are the masses of the longer link and of the foot, h_f and l_f are the hight and lenght of the foot, a and CoP are the location of the ankle (fixed) and center of pressure (not fixed).

2) Compute the backward reachable tube of the target set, including constraints. We call this the *stabilizable region* for sit-to-stand motion.
3) Demonstrate that the stabilizable region, which is also controlled invariant, can be used to analyze the stability of human movement.

IV. METHODS

A. Model and Constraints

Although our formulation is model-agnostic, the inverted pendulum is frequently used as a low dimensional model of human motion and is a good starting point [17]. With generalized coordinates, the state variables of this model are angle and angular velocity, $(\theta, \dot{\theta})$ with model parameters gravitation constant g, mass m, length l, and 'angular' friction constant b. The input is a torque at the ankle, τ, as shown in Figure 1. In first order state space form, we denote the state space $X \subset \mathbb{R}^2$, with $x_1 = \theta, x_2 = \dot{\theta}$ and input τ in input space $U \subset \mathbb{R}$:

$$\begin{bmatrix}\dot{x}_1\\ \dot{x}_2\end{bmatrix} = \begin{bmatrix} x_2 \\ -(\frac{g}{l})\cos(x_1) - (\frac{b}{ml^2})x_2 + (\frac{1}{ml^2})\tau\end{bmatrix}. \quad (3)$$

We assume that there are bounds on the torque, representing the strength of the muscles that produce the ankle torque:

$$\tau_{lb} \leq \tau \leq \tau_{ub}. \quad \text{(C1)}$$

For the underactuated two- link model, we include a link representing the foot of length l_f and mass m_f. To ensure the foot stays flat on the ground, we define the following constraints, similar to [18] and [34]:

$$F_{gy} \geq 0 \quad \text{(C2)}$$

$$\text{CoP} \in \text{BoS}, \quad \text{(C3)}$$

$$|F_{gx}| < \mu F_{gy}. \quad \text{(C4)}$$

F_{gx} and F_{gy} are the ground reaction force in the x and y directions, shown in Figure 1. The coefficient of static friction is μ, CoP is the Center of Pressure, and BoS refers to the Basin of Support, or foot. In the simple planar case, this corresponds to a line segment on the x-axis of length l_f.

Together, these constraints ensure that the foot remains flat on the ground [20]. Letting $c_\theta = \cos(\theta)$ and $s_\theta = \sin(\theta)$, The equation for F_{gx} in terms of the state variables is

$$F_{gx} = ml(-\ddot{\theta}s_\theta - \dot{\theta}^2 c_\theta). \tag{4}$$

The equation for F_{gy} is

$$F_{gy} = m_f g + ml(\ddot{\theta}c_\theta - \dot{\theta}^2 s_\theta) + mg. \tag{5}$$

Given the definitions of F_{gx} and F_{gy}, if we replace $\ddot{\theta}$ with its expression in terms of states from the righthand side of Eq. (3), it is possible to transform constraints (C2)-(C4) into state-dependent constraints on the ankle torque, τ. Derivations of these constraints, along with the equations of motion, are provided in [18].

B. Controlled Invariance of the Target Set

The target set is described with respect to cartesian coordinates in our problem formulation. It is, however, computationally more efficient to compute the controlled invariant set in the lower dimensional polar coordinate representation. We use the dynamics and constraints defined in section IV-A. The angle θ_{min} corresponds to the angle at which the center of mass of the body is over the heel, and θ_{max} for the center of mass over the toe. Figure 1 is approximately in the θ_{min} configuration; it is easy to see that $\theta_{min} = \cos^{-1}(\frac{a}{l})$ and $\theta_{max} = \cos^{-1}(\frac{l_f - a}{l})$. To enforce 0 velocity in the x direction, we restrict angular velocity to be 0. In polar coordinates, our target set Ω_θ is

$$\Omega_\theta = \{x \in X \mid x_1 \in (\theta_{min}, \theta_{max}), x_2 = 0\}. \tag{6}$$

Proposition 2. *The set Ω_θ is controlled invariant. It remains so under constraints* (C1)-(C4) *given sufficiently large torque bounds.*

Proof: To prove the invariance of Ω_θ, it suffices to show that for any initial condition $x_0 \in \Omega_\theta$, a controller exists that causes the system state to remain in Ω_θ for all time.

Choose an arbitrary $x_0 \in \Omega_\theta$, where $x_0 = [\hat{\theta}; 0]$. Within Ω_θ, the dynamics are

$$\tau = mgl^2\ddot{\theta} + mgl\cos\theta. \tag{7}$$

To remain in the set, acceleration must be 0. Otherwise the system velocity will become nonzero and the system state will exit Ω_θ. Observe that by letting

$$\tau = mgl\cos\theta, \tag{8}$$

$\ddot{\theta} = 0$. This implies that the velocity will remain constant at 0, and that the position will remain at $\hat{\theta}$. Thus Ω_θ is controlled invariant in the absence of constraints on τ. Note that (8) is a simple case of an inverse dynamics controller [35, Chapter 8]. It remains to show that the proposed controller does not violate the constraints C1-C4.

Constraint 1: Recall that the angle θ_{min} corresponds to a CoM position above the heel, and θ_{max} above the toe. Because $\theta = \frac{\pi}{2}$ when the CoM position is directly above the ankle, $0 < \theta_{min} < \frac{\pi}{2}$ and $\frac{\pi}{2} < \theta_{max} < \pi$. This means that $\cos\theta_{min} > 0$ and $\cos\theta_{max} < 0$. Thus $\max_\theta \cos\theta = \theta_{min}$ and $\min_\theta \cos\theta = \theta_{max}$. Since parameters $m, g, l > 0$, it is possible to set bounds on the inverse dynamics controller derived previously: $mgl\cos\theta_{max} < \tau < mgl\cos\theta_{min}$. As long as $\tau_{lb} \leq mgl\cos\theta_{max}$ and $\tau_{ub} \geq mgl\cos\theta_{min}$, Ω_θ remains controlled invariant under constraint (C1).

Constraint 2: From equation (5) we see that when CoM velocity and acceleration are 0, the vertical ground reaction force, $F_{gy} = (m+m_f)g$, a positive quantity. As the velocity of the CoM is 0 within Ω_θ, and controller (8) enforces $\ddot{\theta} = 0$, C2 is satisfied.

Constraint 3: The set Ω_θ is defined such that the x coordinate of the CoM (CoM_x) is within the BoS. When the acceleration of the CoM is 0, the CoP location is equivalent to CoM_x [20]. It follows that since $\ddot{\theta} = 0$ with controller (8), $\text{CoP} = \text{CoM}_x \in \text{BoS}$. Thus this controller satisfies constraint (C3).

Constraint 4: When $\dot{\theta} = 0$ and $\ddot{\theta} = 0$, there is no ground reaction force in the x-direction, so $F_{gx} = 0$. Under these same conditions, $F_{gy} = (m+m_f)g$. As μ is always positive, $\dot{\theta} = 0$ within Ω_θ, and controller (8) enforces that $\ddot{\theta} = 0$, constraint (C4) is always satisfied. □

Given that our target set is invariant, in what follows we explain how we compute the backward reachable set of the target set. By Corollary 1, this gives us the reachable tube representing the stabilizable region.

C. Computing the Backward Reachable Set

We use the Hamilton-Jacobi-Bellman (HJB) toolbox to compute the backward reachable set of Ω_θ. This toolbox computes backward reachable sets by solving an HJB PDE [36]. The user provides the toolbox with a target set, an optimal control function, and safety constraints. The solution of the PDE is a function $V(t, x)$, of time and state. At time t, the zero-sublevel of $V(t, x)$ is equivalent to the backward reachable set:

$$\mathcal{G}_t = \{x \mid V(t, x) \leq 0\}. \tag{9}$$

For ease of computation, we relax the definition of our target set Ω_θ and allow a small range of angular velocity $(\dot{\theta}_{min}, \dot{\theta}_{max})$. This can also be interpreted as accounting for postural sway. Our relaxed target set Ω_r is

$$\Omega_r = \{x \in X \mid x_1 \in (\theta_{min}, \theta_{max}), x_2 \in (\dot{\theta}_{min}, \dot{\theta}_{max})\}. \tag{10}$$

This set is no longer controlled invariant. At the extreme corners of the set, for example $x_1 = \theta_{max}$, $x_2 = \dot{\theta}_{max}$, remaining in Ω_r would require an instantaneous change in the direction of the velocity. Inside Ω_r but close to this corner, impossibly high torques would be required to remain within the set. As Ω_r is no longer invariant, the resulting BRS

is also not necessarily invariant. It contains the set of states from which we can reach Ω_r, but there is no guarantee that it is possible to remain in Ω_r. However, we note the following fact.

Fact 2. *Let $\mathcal{G}_T(\Omega_\theta)$ be the controlled invariant backward reachable set that we originally sought to compute, and $\mathcal{G}_T(\Omega_r)$ be the set that we actually compute. Since the original invariant set $\Omega_\theta \subseteq \Omega_r$, we have $\mathcal{G}_T(\Omega_\theta) \subseteq \mathcal{G}_T(\Omega_r)$ for all T.*

We must also provide the optimal control input for a given state. This input is given by the argument of

$$H(t, x, \nabla V) = \min_{u \in U} \nabla V \cdot f(x, u), \tag{11}$$

where $H(t, x, \nabla V)$ is called the Hamiltonian, and function f denotes the appropriate system dynamics. Typically, the optimal control is chosen from a set $U \subset \mathbb{R}^n$. However, our problem includes state-dependent input constraints of the form $u_i \leq h_i(x)$ or $u_i \geq h_i(x)$, where $h_i : X \to \mathbb{R}$ is a function of the states.

Let $U(x)$ denote the set of control values that are allowable for a given state. Then the argument of the equation (11) with the input-affine dynamics from (3) is given by

$$\tau^* = \arg \min_{\tau \in U(\hat{x})} \frac{\partial V(t, \hat{x})}{\partial \hat{x}_2} \frac{1}{ml^2} \tau, \tag{12}$$

where the quantity $\frac{\partial V(t,\hat{x})}{\partial \hat{x}_2}$ is computed by the HJB solver. Since $\tau \in \mathbb{R}$, only two state-dependent input constraints can be 'active' at $\hat{x}$, representing upper and lower bounds. We denote these constraints $h_a^-(\hat{x})$ and $h_a^+(\hat{x})$. Thus $\tau^* = h_a^+(\hat{x})$ if $\frac{\partial V(t,\hat{x})}{\partial \hat{x}_2} < 0$ and $\tau^* = h_a^-(\hat{x})$ otherwise.

Finally, the state-dependent input constraints described in the previous sections delimit the safe subset of the state space where a valid input u exists. We provide the toolbox with the boundaries of this set. For details of how to handle state-dependent input constraints in HJB framework, see [37].

V. RESULTS

A. Stabilizable Regions for Varying Parameters

To compare directly with the results of [18], we use the same model parameters, with $m = 80\,\mathrm{kg}$ and $l = 1.78\,\mathrm{m}$. The ankle torque bounds are $-142\,\mathrm{N \cdot m}$ for plantarflexion (foot rotation away from anterior leg) and $43.3\,\mathrm{N \cdot m}$ for dorsiflexion (foot rotation toward anterior leg), which are mean bounds reported for males in muscle strength studies of healthy populations [38]. The velocity tolerances for the target set (10) are $(-0.1\,\mathrm{rad/sec}, 0.1\,\mathrm{rad/sec})$. Additional parameters such as foot length were approximated as percentages of height based on anthropometric data, as in [18].

We compute the backwards reachable tube of the target set over a time horizon of 1.5 seconds as this is sufficient for the computation to converge. The resulting stabilizable region computed under nominal (high friction) conditions can be seen in Figure 2, in the lightest gray color. We plot our results in terms of x-position and velocity of the CoM, to directly compare with [18], [19]. We use the same convention

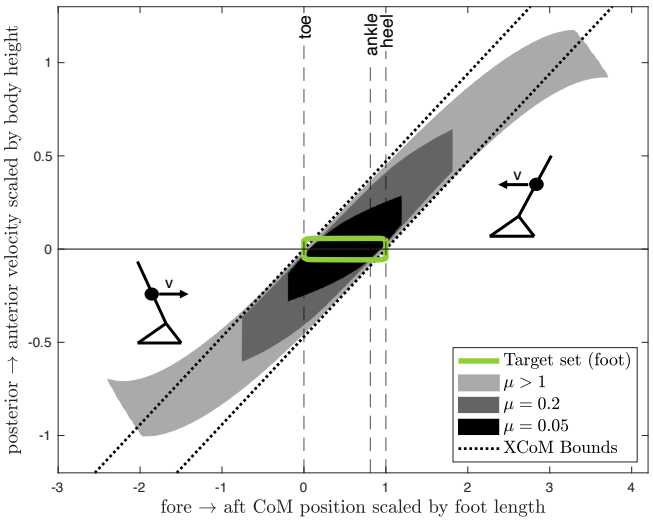

Fig. 2: Stabilizable region of the two-link inverted pendulum model under varying friction conditions are shown in shades of gray. The target set representing the CoM position over the foot at low velocity is in green. The boundaries of the XCoM method, which cannot account for friction, are shown as well via dashed lines. The stick figures indicate the CoM position and the direction of the CoM velocity within relevant regions of the figure.

of positive velocity corresponding to anterior motion in the direction from the heel to the toe. We find that the upper and lower boundaries of our stabilizable region approximately match the boundaries in [18]. For example, at 2.4 foot lengths behind the heel, the upper bound on the velocity is approximately 1.1 m/s (scaled by body height), as computed in [18]. Notably, our stabilizable regions include the portion of the state space corresponding to velocities in the posterior direction. This would be of relevance during motions such as single leg balance, and was not included in [18], likely due to computational issues.

The effect of varying the friction constraint parameter μ is shown in Figure 2. As μ decreases, we expect the region to decrease in size; the figure supports this observation. Similarly, decreasing the size of the BoS or reducing the absolute torque bounds also results in a smaller stabilizable region (not shown).

For reference, we also include the bounds computed using the popular XCoM method [19], shown as dotted lines in Figure 2. Because the XCoM bounds are computed using a linear model, they provide a good local estimate around the target set. However the XCoM method cannot capture variations in parameters such as friction or biological torque bounds, which represent factors such as different environments and loss of strength due to aging or disease.

B. Preliminary Validation with Experimental Data

To perform a preliminary exploration of the stabilizable region with human subject data, we use the dataset described in [24] and compare our results with the stability basin method introduced in the same paper. This dataset includes

movement trajectories of 11 subjects performing sit-to-stand. External perturbations are applied during certain trials to induce 'failures' where the subject must take a step or sit back down. Perturbations are applied either forwards or backwards via a cable pull in the anterior-posterior direction. We specifically consider perturbed sit-to-stand trajectories performed using a natural strategy, where no specific instructions were provided to participants regarding execution of the movement. Because the boundaries of the stabilizable region depend on model parameters, we compute personalized regions for each participant using their height and mass. Parameters such as foot length, ankle location, and torque bounds are not provided, so we compute approximations using anthropomorphic data as described in the previous section.

Subjects were not told to try to avoid taking a step or sitting back down. Thus this dataset provides examples of 'failed' trajectories, where it is unclear whether the subject could have used an alternative control strategy to avoid failure. Because our formulation maximally includes all possible control strategies, it may provide a way to differentiate between these cases. In a case where an alternative strategy exists, we would expect the perturbed trajectory to exit the stabilizable region *after* the perturbation is applied. When the perturbation actually causes an unrecoverable failure, the trajectory should exit the set *during* the perturbation. Examples of both these types of trajectories are plotted in Figure 3.

Of the perturbed trials in the dataset, 71 resulted in the subject taking a step forwards or backwards, or sitting back on the chair. Of these, 29 resulted in the subject having to sit back in the chair. It is reasonable to assume that such sit-back failures are more likely to occur when no control strategy exists to overcome the applied perturbation. Focusing on these specific trials, we find that the end of the perturbation occurs outside or on the boundary of the stabilizable region in $26/29$ trials. In comparison, the perturbed portion of the trajectory exits the stability basin $12/29$ times for the same subset of trials. Of the 42 trials, in which the subject to took a step, 22 exit the stabilizable region during perturbation while 9 exit the stability basin. Results are summarized in Table I.

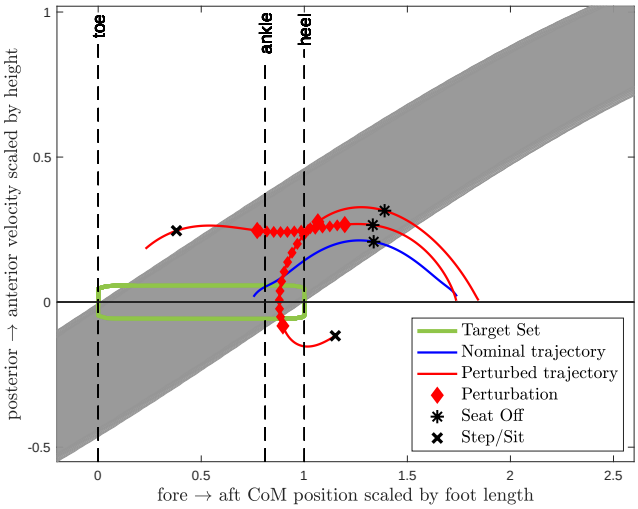

Fig. 3: An unperturbed sit-to-stand trial in blue plotted along side two perturbed trials. The stabilizable region is in gray. The moment when the step was taken is indicated by the black 'x.'Perturbation was applied continuously between the red diamond markers. One perturbed trajectory exits the stabilizable region during the perturbation, while the other exits the set after. This illustrates a possible true failure case vs a situation where an alternative control strategy might have allowed the participant to maintain balance.

	Method	Pert. End Out	In
Sit-back	SR	$26/29\,(90\%)$	$3/29\,(10\%)$
	SB	$12/29\,(41\%)$	$17/29\,(59\%)$
Step	SR	$22/42\,(52\%)$	$20/42\,(48\%)$
	SB	$9/42\,(21\%)$	$33/42\,(79\%)$

TABLE I: Comparison of our stabilizable region method (SR) and the stability basin method from [24](SB). We look at trials that resulted in the subject sitting back on the chair (Sit-back) and trials where the subject to a step forward or backward (Step). For each outcome, we look at whether the perturbed portion of the trajectories exit the stability bounds computed by each method during the perturbation (Out) or after the perturbation is complete (In).

VI. Discussion and Future Work

The results with respect to sit-back failures indicate that the stabilizable region may be better able to characterize true failures than the stability basin method. This is likely because the torque bounds used to compute the stability basins are learned from nominal, forward moving sit-to-stand trajectories, and do not account for the differing biomechanics of motion in the opposite direction. In particular, at the moment a subject falls back to their heels, they cannot apply a stabilizing ankle torque. Thus the stability basin method assumes that a fairly large torque can be applied when it cannot. For perturbed trajectories resulting in a step failure, it is harder to make assumptions about the subject's control strategy. However, the lower number of trajectories exiting the bounds during perturbation may indicate that a stepping strategy is often employed even when not strictly necessary. These results are illustrative, as the experiment in [24] was not designed to produce a range of unambiguous sit-to-stand failures. Future work should include experiments that are designed with this goal in mind.

The current model can only reflect two modes of human reaction to perturbation: adjusting foot contact with the ground and using ankle torque to stabilize [39]. The addition of another link would allow the exploration of strategies involving the hip. It will also be of interest to apply our method to the analysis of systems that includes the dynamics of assistive devices, such as an ankle exoskeleton. Unlike prior work, we are able to include such variations in system

dynamics. Our method can also be extended to include physiological state variables related to muscle activation dynamics.

Lastly, endowing the stabilizable region with a metric that can quantify stability is a compelling research direction. Currently available metrics have been shown to have limited experimental validity [21]. Several aspects of HJB reachability may be useful here, particularly the implicit function representation of the reachable sets.

REFERENCES

[1] S. M. Bradley, "Falls in older adults," *Mount Sinai Journal of Medicine*, vol. 78, no. 4, pp. 590–595, 2011.

[2] L. A. Talbot, R. J. Musiol, E. K. Witham, and E. J. Metter, "Falls in young, middle-aged and older community dwelling adults: perceived cause, environmental factors and injury," *BMC Public Health*, vol. 5, no. 1, p. 86, 2005.

[3] H. Cho, M. J. H. Heijnen, B. A. Craig, and S. Rietdyk, "Falls in young adults: The effect of sex, physical activity, and prescription medications," *PLOS ONE*, vol. 16, pp. 1–19, 04 2021.

[4] E. DuPree, A. Fritz-Campiz, and D. Musheno, "A new approach to preventing falls with injuries," *Journal of Nursing Care Quality*, vol. 29, no. 2, 2014.

[5] J. A. Stevens, P. S. Corso, E. A. Finkelstein, and T. R. Miller, "The costs of fatal and non-fatal falls among older adults," *Injury Prevention*, vol. 12, no. 5, pp. 290–295, 2006.

[6] P. M. Dall and A. Kerr, "Frequency of the sit to stand task: An observational study of free-living adults," *Applied Ergonomics*, vol. 41, no. 1, pp. 58 – 61, 2010.

[7] A. Kralj, R. Jaeger, and M. Munih, "Analysis of standing up and sitting down in humans: Definitions and normative data presentation," *Journal of Biomechanics*, vol. 23, no. 11, pp. 1123 – 1138, 1990.

[8] L. Nyberg and Y. Gustafson, "Patient falls in stroke rehabilitation," *Stroke*, vol. 26, no. 5, pp. 838–842, 1995.

[9] S. Lord, S. Murray, K. Chapman, B. Munro, and A. Tiedemann, "Sit-to-stand performance depends on sensation, speed, balance, and psychological status in addition to strength in older people," *The journals of gerontology, series A.*, vol. 57, pp. M539–43, 09 2002.

[10] Y.-C. Pai, F. Yang, J. D. Wening, and M. J. Pavol, "Mechanisms of limb collapse following a slip among young and older adults," *Journal of Biomechanics*, vol. 39, no. 12, pp. 2194–2204, 2006.

[11] B. Najafi, K. Aminian, F. Loew, Y. Blanc, and P. Robert, "Measurement of stand-sit and sit-stand transitions using a miniature gyroscope and its application in fall risk evaluation in the elderly," *IEEE Transactions on Biomedical Engineering*, vol. 49, no. 8, pp. 843–851, 2002.

[12] Y. Lajoie and S. Gallagher, "Predicting falls within the elderly community: comparison of postural sway, reaction time, the berg balance scale and the activities-specific balance confidence (abc) scale for comparing fallers and non-fallers," *Archives of Gerontology and Geriatrics*, vol. 38, no. 1, pp. 11–26, 2004.

[13] C. McCrum, T. Bhatt, M. Gerards, K. Karamanidis, M. Rogers, S. R. Lord, and Y. Okubo, "Perturbation-based balance training: Principles, mechanisms and implementation in clinical practice," *OSF Preprints*, vol. 9, 2022.

[14] T. Voss, J. Elm, C. Wielinski, M. Aminoff, D. Bandyopadhyay, K. Chou, L. Sudarsky, and B. Tilley, "Fall frequency and risk assessment in early parkinson's disease," *Parkinsonism & Related Disorders*, vol. 18, no. 7, pp. 837–841, 2012.

[15] R. Gregg and U. Topcu, "Towards formal verification methods for robotic lower-limb prostheses and orthoses," in *CPS Week Medical Cyber Physical Systems Workshop*, 2013.

[16] O. Narvaez-Aroche, A. Packard, P.-J. Meyer, and M. Arcak, "Reachability analysis for robustness evaluation of the sit-to-stand movement for powered lower limb orthoses," vol. 1 of *Dynamic Systems and Control Conference*, 09 2018. V001T07A006.

[17] D. Winter, "Human balance and posture control during standing and walking," *Gait & Posture*, vol. 3, no. 4, pp. 193–214, 1995.

[18] Y.-C. Pai and J. Patton, "Center of mass velocity position predictions for balance control," *Journal of Biomechanics*, vol. 30, no. 4, pp. 347 – 354, 1997.

[19] A. Hof, M. Gazendam, and W. Sinke, "The condition for dynamic stability," *Journal of Biomechanics*, vol. 38, no. 1, pp. 1–8, 2005.

[20] C. Mummolo, L. Mangialardi, and J. H. Kim, "Numerical Estimation of Balanced and Falling States for Constrained Legged Systems," *Journal of Nonlinear Science*, vol. 27, pp. 1291–1323, Aug. 2017.

[21] S. M. Bruijn, O. G. Meijer, P. J. Beek, and J. H. van Dieën, "Assessing the stability of human locomotion: a review of current measures," *Journal of The Royal Society Interface*, vol. 10, no. 83, p. 20120999, 2013.

[22] P. Zaytsev, W. Wolfslag, and A. Ruina, "The boundaries of walking stability: Viability and controllability of simple models," *IEEE Transactions on Robotics*, vol. 34, no. 2, pp. 336–352, 2018.

[23] N. S. Patil, J. B. Dingwell, and J. P. Cusumano, "Viability, task switching, and fall avoidance of the simplest dynamic walker," *Scientific Reports*, vol. 12, no. 1, p. 8993, 2022.

[24] P. D. Holmes, S. M. Danforth, X.-Y. Fu, T. Y. Moore, and R. Vasudevan, "Characterizing the limits of human stability during motion: perturbative experiment validates a model-based approach for the sit-to-stand task," *Royal Society Open Science*, vol. 7, no. 1, p. 191410, 2020.

[25] Z. Liu and N. Ozay, "On the convergence of the backward reachable sets of robust controlled invariant sets for discrete-time linear systems," in *61st IEEE Conference on Decision and Control*, 2022.

[26] Y. Li and J. Liu, "ROCS: A robustly complete control synthesis tool for nonlinear dynamical systems," in *Proc. of the 21st HSCC*, pp. 130–135, 2018.

[27] S. Bansal, M. Chen, S. Herbert, and C. J. Tomlin, "Hamilton-Jacobi reachability: A brief overview and recent advances," in *2017 IEEE 56th Conf. on Decision and Control*, pp. 2242–2253, 2017.

[28] G. Pola, A. Girard, and P. Tabuada, "Approximately bisimilar symbolic models for nonlinear control systems," *Automatica*, vol. 44, no. 10, pp. 2508–2516, 2008.

[29] M. Korda, D. Henrion, and C. N. Jones, "Convex computation of the maximum controlled invariant set for polynomial control systems," *SIAM Journal on Control and Optimization*, vol. 52, no. 5, pp. 2944–2969, 2014.

[30] P. Saint-Pierre, "Approximation of the viability kernel," *Applied Mathematics and Optimization*, vol. 29, no. 2, pp. 187–209, 1994.

[31] E. Goubault and S. Putot, "Inner and outer reachability for the verification of control systems," in *Proc. of the 22nd HSCC*, pp. 11–22, 2019.

[32] L. Yang, H. Zhang, J.-B. Jeannin, and N. Ozay, "Efficient backward reachability using the minkowski difference of constrained zonotopes," *IEEE Transactions on Computer-Aided Design of Integrated Circuits and Systems*, 2022.

[33] B. Schurmann, M. Klischat, N. Kochdumper, and M. Althoff, "Formal safety net control using backward reachability analysis," *IEEE Transactions on Automatic Control*, 2021.

[34] M. Vukobratovic and B. Borovac, "Zero-moment point - thirty five years of its life.," *I. J. Humanoid Robotics*, vol. 1, pp. 157–173, 03 2004.

[35] M. Spong, S. Hutchinson, and M. Vidyasagar, *Robot Modeling and Control*. Wiley select coursepack, Wiley, 2005.

[36] I. Mitchell, "A toolbox of level set methods," Tech. Rep. TR-2007-11, University of British Columbia, Department of Computer Science, June 2007.

[37] S. Bortoletto, "The Bellman equation for constrained deterministic optimal control problems," *Differential and Integral Equations*, vol. 6, no. 4, pp. 905–924, 1993.

[38] B. Danneskiold-Samsøe, E. M. Bartels, P. M. Bulow, H. Lund, A. Stockmarr, C. C. Holm, I. Wattjen, M. Appleyard, and H. Bliddal, "Isokinetic and isometric muscle strength in a healthy population with special reference to age and gender," *Acta Physiologica*, vol. 197, no. s673, pp. 1–68, 2009.

[39] F. B. Horak, "Postural orientation and equilibrium: what do we need to know about neural control of balance to prevent falls?," *Age and Ageing*, vol. 35, pp. ii7–ii11, 09 2006.